www.czasopisma.pan.pl PAN www.journals.pan.pl
Opto-Electronics Review 26 (2018) 188–193

Contents lists available at ScienceDirect

Opto-Electronics Review

journal homepage: http://www.journals.elsevier.com/opto-electronics review

Full Length Article

MW peak power KTP-OPO-based "eye-safe" transmitter

M. Kaskow, L. Gorajek*, W. Zendzian, J. Jabczynski

Military University of Technology, 2 Gen.W. Urbanowicza Str., 00-908 Warsaw, Poland

ARTICLE INFO

Article history:
Received 10 November 2017
Received in revised form 16 April 2018
Accepted 20 April 2018
Available online 29 May 2018

Keywords:
Optical parametric oscillator
Q-switched laser
Neodymium laser

ABSTRACT

We demonstrate MW-level, single resonance optical parametric oscillator, based on KTP Type-II crystal with noncritical phase-matching. The OPO is pumped by electro-optically Q-switched Nd:YAG slab laser providing 55 mJ of pulse energy. At the output, we achieved 28 mJ of signal pulse energy at 1.57 μm with 51% conversion efficiency, corresponding to 1.4 MW of peak power.

1. Introduction

The "eye-safe" devices generating laser radiation in a 1.5 μm range are commonly used in various types of applications. The most demanding and challenging one is the military equipment. It requires laser sources to be very robust, durable and easy-to-use in fast-changing battlefield conditions. The most promising gain media for this kind of generators are erbium-doped fibres [1,2] and erbium doped crystals [3,4]. Fibre lasers enable high power scaling with near-diffraction-limited output beams. Very high surface-to-volume ratio provides excellent thermal management capabilities. Moreover, fibre components are so widely available, that processing lead time of laser generator can be minimized. Despite many advantages, EDFAs have one serious drawback – inoperability in generation with high pulse energy and ns-pulse duration. The power density at the fibre ends is extremely high and it causes fractures. To achieve high peak power output, one must design a slab- or rod-based solid-state laser or parametric oscillators (OPO) [5–8].

In this paper we demonstrate an "eye-safe" optical-parametric oscillator based on a KTP crystal pumped by diode-side-pumped, Q-switched Nd:YAG slab laser. The KTP-OPO generates a single pulse with an energy of 28 mJ with 20 ns pulse duration.

2. Why KTP crystal for Nd:YAG pumped optical parametric oscillator?

The KTP crystal is a well-known non-linear medium for second harmonic generation in Nd-doped lasers, mostly due to its high non-linear coefficient (d_{eff} = 3.65 pm/V) and high damage threshold. Commercially available media have LIDT values around 2.4 GW/cm^2 and 4.6 GW/cm^2 [9] for 10 ns and 1.3 ns long pulses at 1064 nm wavelength, respectively. The transmission range covers wide 0.35–4.5 μm spectrum. It is worth mentioning, that one may apply KTA medium instead. However, despite having 1.5× larger d_{eff} and lower intrinsic losses in a 3 μm range, commercially available KTA crystals are offered in a 3 lengths below 30 mm. The detailed comparison between KTP and KTA can be found in Ref. [10]. KTP is an anisotropic, biaxial, positive nonlinear crystal with main crystallographic axes X, Y, Z ($n_z > n_y > n_x$). To calculate refractive indices at certain wavelength, one may evaluate KTP Sellmeier equations at 25 °C [9,11]:

$$\begin{aligned} n_x^2 &= 3.0065 + \frac{0.03901}{\lambda^2 - 0.04251} - 0.01327 \cdot \lambda^2 \\ n_y^2 &= 3.0333 + \frac{0.04154}{\lambda^2 - 0.04547} - 0.01408 \cdot \lambda^2 \\ n_z^2 &= 3.3134 + \frac{0.05694}{\lambda^2 - 0.05658} - 0.01682 \cdot \lambda^2 \end{aligned} \quad (1)$$

For example: for λ = 1.064 μm – n_x = 1.7377, n_y = 1.7453, n_z = 1.8297. Because of $n_z > n_y > n_x$, the KTP optical axes lay in XZ plane and form with Z-axis an angle β_z = 17.4°.

$$\tan\beta_z = \frac{n_z}{n_x}\sqrt{\frac{{n_y}^2 - {n_y}^2}{{n_z}^2 - {n_y}^2}} \quad (2)$$

In anisotropic medium, the refractive indices for two orthogonal, linearly polarized waves propagating along ***s*** versor

* Corresponding author.
E-mail address: lukasz.gorajek@wat.edu.pl (L. Gorajek).

https://doi.org/10.1016/j.opelre.2018.04.005

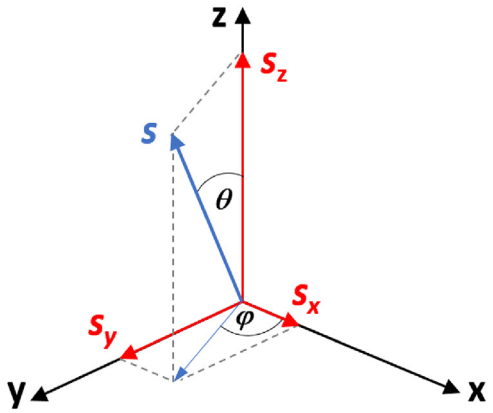

Fig. 1. The ***s*** versor components.

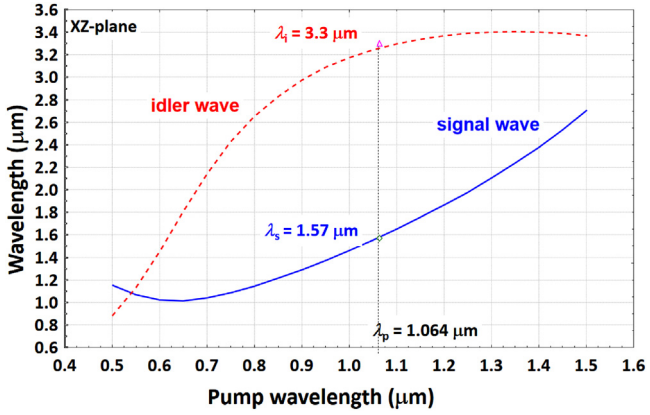

Fig. 2. Signal and idler wavelengths as a function of pump wavelength.

(perpendicular to its wavefront), can be calculated by means of Fresnel equation [12,13]:

$$\frac{s_x{}^2}{\frac{1}{n(\theta,\varphi)^2}-\frac{1}{n_x{}^2}}+\frac{s_y{}^2}{\frac{1}{n(\theta,\varphi)^2}-\frac{1}{n_y{}^2}}+\frac{s_z{}^2}{\frac{1}{n(\theta,\varphi)^2}-\frac{1}{n_z{}^2}}=0 \tag{3}$$

The s_x, s_y, s_z components create with OZ and OX axes θ and φ angles, respectively (see Fig. 1):

$$\begin{aligned} s_x &= \sin\theta\cos\varphi \\ s_y &= \sin\theta\sin\varphi \\ s_z &= \cos\theta \end{aligned} \tag{4}$$

Introducing Eq. (4) into Eq. (3), after a short derivation we obtain:

$$s_x{}^2\left(\frac{1}{n^2}+\frac{1}{n_y{}^2}\right)\left(\frac{1}{n^2}+\frac{1}{n_z{}^2}\right)+s_y{}^2\left(\frac{1}{n^2}+\frac{1}{n_x{}^2}\right)\left(\frac{1}{n^2}+\frac{1}{n_z{}^2}\right)+s_z{}^2\left(\frac{1}{n^2}+\frac{1}{n_y{}^2}\right)\left(\frac{1}{n^2}+\frac{1}{n_y{}^2}\right)=0 \tag{5}$$

Eq. (5) has two solutions for two orthogonally-polarized waves:

$$\begin{aligned} \frac{1}{n_1(\theta,\varphi)^2} &= \frac{b+\sqrt{b^2-4c}}{2} \\ \frac{1}{n_2(\theta,\varphi)^2} &= \frac{b-\sqrt{b^2-4c}}{2} \end{aligned} \tag{6}$$

where:

$$b = s_x{}^2\left(\frac{1}{n_y{}^2}+\frac{1}{n_z{}^2}\right)+s_y{}^2\left(\frac{1}{n_x{}^2}+\frac{1}{n_z{}^2}\right)+s_z{}^2\left(\frac{1}{n_x{}^2}+\frac{1}{n_y{}^2}\right) \tag{7}$$

$$c = s_x{}^2\frac{1}{n_y{}^2n_z{}^2}+s_y{}^2\frac{1}{n_x{}^2n_z{}^2}+s_z{}^2\frac{1}{n_x{}^2n_y{}^2} \tag{8}$$

Be advised, that in case of biaxial crystals, the optical indicatrix cross-section (perpendicular to ***s*** versor) is an ellipse. The ellipse axes lengths are equal to the refractive indices values of two linearly polarized waves, and are expressed by Eqs. (6)–(8).

If the interacting waves propagate along one of the main axes X, Y or Z, the "walk-off" effect does not occur. Let the waves propagate in XZ plane in OX direction. In this case, $s_y = s_z = 0$, $s_x = 1$, and Eq. (5) has two solutions: $n_1(90^\circ,0^\circ) = n_y$ and $n_2(90^\circ,0^\circ) = n_z$. The refractive index of two waves polarized in OZ- and OY-direction is equal to n_z and n_y, respectively.

The phase-matching condition can be fulfilled if one of the interacting waves, propagating in the OX direction, is orthogonally-polarized to the two others. The numerical analysis of the problem indicates, that the best solution can be only achieved, when pump and signal waves are linearly-polarized in OY-direction and idler wave is polarized in OZ-direction. Phase-matching condition is expressed as follows:

$$\begin{aligned} \frac{\lambda_p}{\lambda_s}n_y(\lambda_s)+\frac{\lambda_p}{\lambda_i}n_z(\lambda_i) &= n_y\left(\lambda_p\right) \\ \frac{1}{\lambda_s}+\frac{1}{\lambda_i} &= \frac{1}{\lambda_p} \end{aligned} \tag{9}$$

where: λ_p – pump wavelength: λ_s – signal wavelength, λ_i – idler wavelength. Numerical solutions of Eq. (9), taking into account Sellmeier equations, are presented in Fig. 2. For pump wavelength $\lambda_p = 1.064$ μm, the signal wave is equal to $\lambda_s = 1.57$ μm, whereas the idler wave $\lambda_i = 3.3$ μm.

The above analysis results in two important conclusions:

1) non-critical phase-matching in KTP for pump wavelength $\lambda_p = 1.064$ μm is fulfilled for "eye-safe" signal wave $\lambda_s = 1.57$ μm and idler wave $\lambda = 3.3$ μm,
2) KTP should be cut along OX-axis in such manner, that its two sidewalls are parallel to XZ-plane.

In this particular case, the energy of pump wavelength (polarized in OY-direction) will be efficiently transferred to both signal wave (with the same polarization) and idler wave (polarized in OZ-direction). The KTP length is limited only by the growth technology. The KTP crystals are commercially available with lengths up to 40 mm.

Let us analyse the influence of KTP and OPO resonator axes collinearity error. We must examine phase-matching condition by varying θ and φ angles. As the first scenario, let us consider three interacting waves propagating in XZ-plane at an angle θ to OZ-axis ($\varphi = 0^\circ$). It will allow us to get an answer to the question: what is the influence of KTP rotation in XZ-plane? Because $s_x = \sin\theta$, $s_y = 0$ and $s_z = \cos\theta$, Eq. (3) becomes:

$$\frac{\sin^2\theta}{n(\theta)^{-2}-n_x{}^{-2}}+\frac{\cos^2\theta}{n(\theta)^{-2}-n_z{}^{-2}}=0 \tag{10}$$

After simple derivation, we obtain:

$$n\left(\theta\right) = \left(\frac{1}{n_x{}^{-2}+\left(n_z{}^{-2}-n_x{}^{-2}\right)\sin^2\theta}\right)^{\frac{1}{2}} \tag{11}$$

For example, for angle $\theta = \pi/2$ and the wave with electrical induction vector oscillating in XZ-plane, the refractive index is

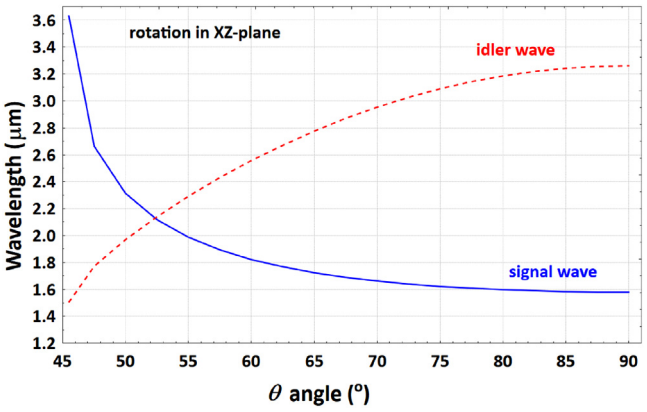

Fig. 3. Signal and idler wavelengths as a function of θ angle (pump wavelength 1.064 μm).

equal to $n(\pi/2) = n_z$. Introducing Eq. (11) into Eq. (9), the new phase-matching condition is expressed by Eq. (12):

$$\frac{\lambda_p}{\lambda_s} n_y(\lambda_s) + \frac{\lambda_p}{\lambda_i} n(\theta, \lambda_i) = n_y(\lambda_p)$$
$$\frac{1}{\lambda_s} + \frac{1}{\lambda_i} = \frac{1}{\lambda_p} \tag{12}$$

The numerical solution of Eq. (12), taking into account Fresnel and Sellmeier equations, is shown in Fig. 3. The pump wavelength is 1.064 μm.

The result clearly shows, that wavelengths generated in a non-critical KTP-OPO is not very sensitive to in angle-tuning in XZ-plane. The θ change in the range of $90^\circ \pm 5^\circ$ changes the signal wavelength by ca. 9 nm. The KTP and OPO resonator axes collinearity error of 1° (in XZ-plane) detunes the signal wavelength by 0.28 nm, whereas idler wavelength is detuned by 1.2 nm.

Let us consider now the second scenario, where the waves propagate in XY-plane at an angle φ to OX-axis ($\theta = 90^\circ$). It will help us to obtain an answer to second question: what is the influence of KTP rotation in XY-plane on OPO properties? In this case, the ***s*** versor components are expressed as follows: $s_x = \cos\varphi$, $s_y = \sin\varphi$, $s_z = 0$, and Eq. (3) becomes:

$$\frac{\sin^2\varphi}{n(\varphi)^{-2} - n_y{}^{-2}} + \frac{\cos^2\varphi}{n(\varphi)^{-2} - n_x{}^{-2}} = 0 \tag{13}$$

After few simple derivations, we obtain

$$n(\varphi) = \left(\frac{1}{n_y{}^{-2} + \left(n_x{}^{-2} - n_y{}^{-2}\right) \sin^2\varphi} \right)^{\frac{1}{2}} \tag{14}$$

For example, for angle $\varphi = 0$ and the wave with electric displacement field vector ***D*** oscillating in XY-plane, the refractive index is equal to $n(0) = n_y$. The phase-matching condition is modified and becomes:

$$\frac{\lambda_p}{\lambda_s} n(\lambda_s, \varphi) + \frac{\lambda_p}{\lambda_i} n_z(\lambda_i) = n_y(\lambda_p, \varphi)$$
$$\frac{1}{\lambda_s} + \frac{1}{\lambda_i} = \frac{1}{\lambda_p} \tag{15}$$

The numerical solution of Eq. (15) is presented below in Fig. 4.

According to the obtained results, the non-critical KTP-OPO angle-tuning in XY-plane is much less sensitive than in XZ-plane case. The φ angle variation of $0^\circ \pm 5^\circ$ causes signal wavelength change of ca. 1 nm. Collinearity error of 1° detunes the signal wavelength only by 0.28 nm, whereas idler wavelengths is detuned by 1.2 nm. The KTP and OPO resonator axes collinearity error of 1°

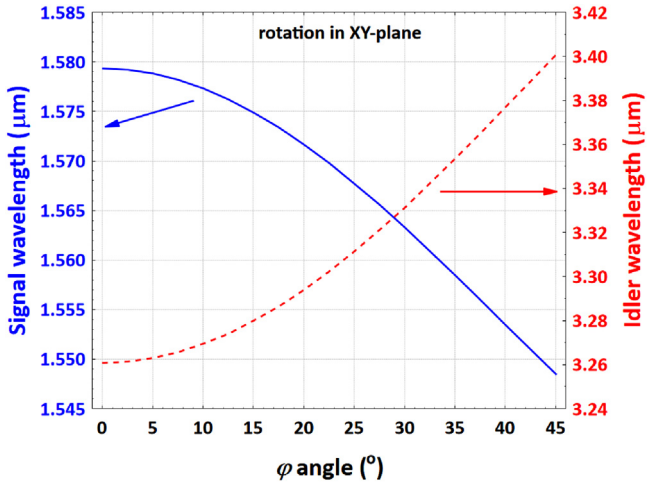

Fig. 4. Signal and idler wavelengths as a function of φ angle (pump wavelength 1.064 μm).

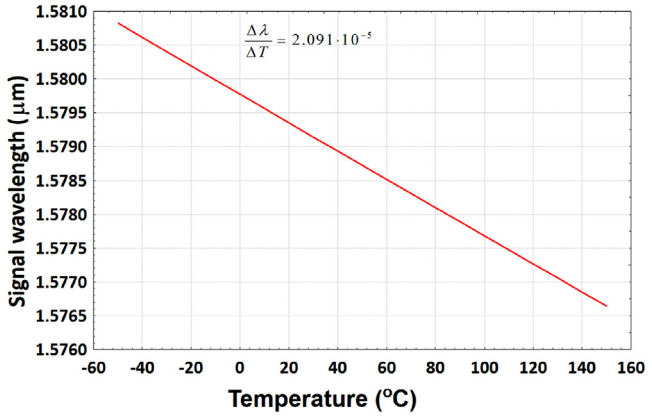

Fig. 5. KTP-OPO signal wavelength as a function of KTP temperature – pump wavelength 1.064 μm.

(in XY-plane) changes the signal and idler wavelengths only by 0.03 nm and 0.14 nm, respectively.

The analysis clearly shows, that KTP-based optical parametric oscillator is very resistant to misalignment of KTP and OPO resonator axes. Moreover, the presented characteristics indicate, that the angle tuning of generated wavelengths is very inefficient in this configuration.

Let us analyse the influence of KTP temperature on signal wavelength. We must numerically evaluate Eq. (9), considering Eq. (1) and taking into account KTP thermal dispersion coefficients [9]:

$$\frac{dn_x}{dT} = 1.1 \cdot 10^{-5} \frac{1}{^\circ C}$$

$$\frac{dn_y}{dT} = 1.3 \cdot 10^{-5} \frac{1}{^\circ C}$$

$$\frac{dn_z}{dT} = 1.6 \cdot 10^{-5} \frac{1}{^\circ C}$$

The solution is shown below in Fig. 5.

One can see, that temperature change in the range of $-50\,^\circ C \div 150\,^\circ C$ causes the signal wavelength change of 1.5808 μm ÷ 1.5767 μm – approximately 4 nm. It is very important for military applications. The research demonstrated in Ref. [14]

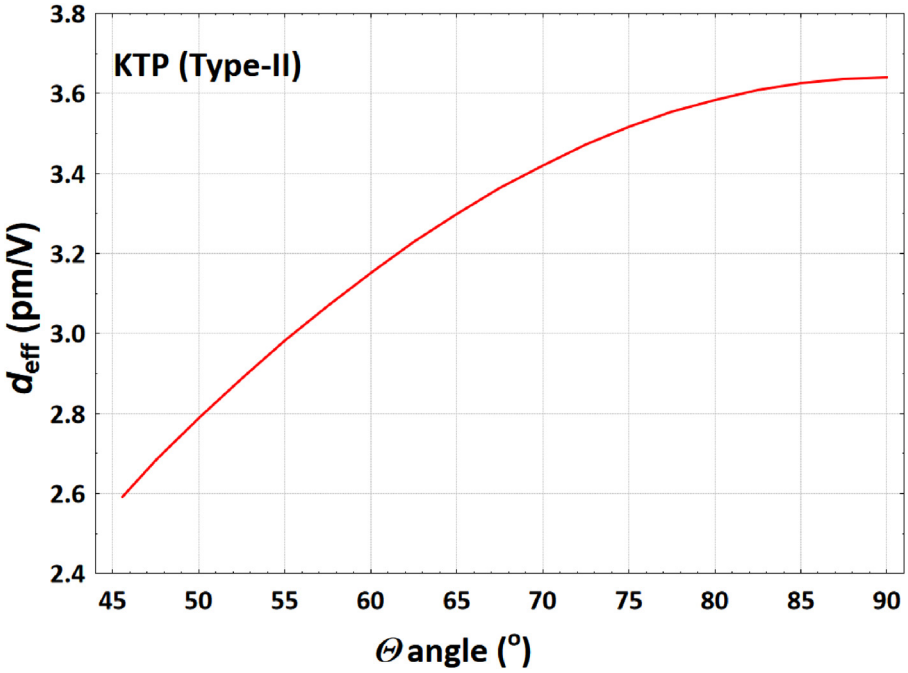

Fig. 6. Effective nonlinear coefficient d_{eff} as a function of angle θ – pump wavelength 1.064 μm.

confirms our theoretical analysis. The KTP nonlinear coefficients d_{ij} values are as follows [15]:

$$d_{15} = 1.91\,pm/V$$

$$d_{24} = 3.64\,pm/V$$

$$d_{31} = 2.54\,pm/V$$

$$d_{32} = 4.35\,pm/V$$

$$d_{33} = 16.9\,pm/V$$

In case of KTP Type-II interaction, where signal and idler waves are orthogonally polarized, the efficient nonlinear coefficient d_{eff} is expressed by [10,15]:

$$d_{eff}\,(II) \approx (d_{24} - d_{15})\sin 2\varphi\,\sin 2\theta - \left(d_{15}\sin^2\varphi + d_{24}\cos^2\varphi\right)\sin\theta \tag{16}$$

The detailed information of how to determine d_{eff} in uniaxial anisotropic crystals can be found in [16]. In case of biaxial media, more details are described in Refs. [17,18]. The dependency of d_{eff} as a function of $\theta(\varphi = 0)$ and $\varphi(\theta = 0)$ angles is shown in Figs. 6 and 7, respectively.

Please note, that for non-critical phase-matching $\theta = 90^\circ$ and $\varphi = 0^\circ$, efficient nonlinear coefficient reaches maximum value and is equal to $d_{\text{eff}} = 3.64$ pm/V, but is 4.6 × smaller than d_{33}. To fully benefit from maximum d_{ij}, one must apply quasi-phase-matching (QPM).

3. Experimental setup

The KTP-OPO was pumped by a Q-switched Nd:YAG slab laser. The resonator scheme is shown in Fig. 8.

Two mirrors: M_1 (HR@1.064 μm, r = 2 m; *LAYERTEC*) and output mirror M_{OC} ($T_{OC} = 60\%$) formed a linear resonator. The 1% Nd:YAG

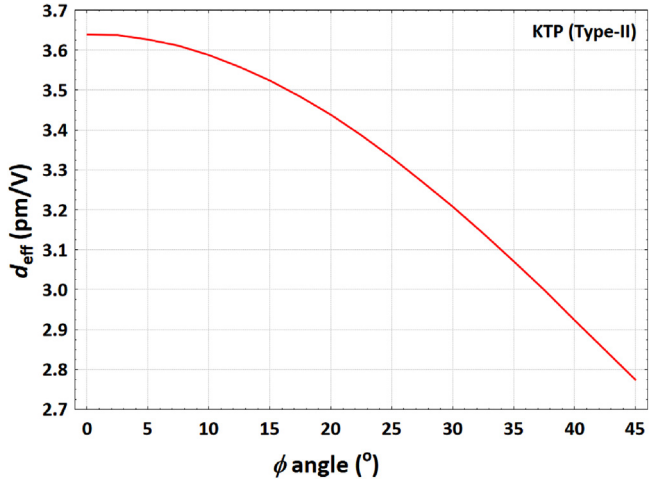

Fig. 7. Effective nonlinear coefficient d_{eff} as a function of angle φ – pump wavelength 1.064 μm.

monocrystalline active medium with dimensions of $4 \times 4 \times 50\ mm^3$ was pumped from two opposite sides by two 2D laser diode arrays (LDA; *DILAS*), separated longitudinally by 15 mm. The Nd:YAG facets were cut parallel at certain angle. It provided two TIRs of the resonator mode in the regions with highest gain (see Fig. 9).

It also acted as a gain-aperture – spatially filtering the transverse resonator mode. The two opposite pumping sides were AR coated at 0.8–0.82 μm, whereas two other sides were ground in order to supress parasitic oscillations. Two front facets of a slab were AR coated at 1.064 μm. The LDAs provided up to 4 kW of pump peak power in a pulse duration of 0.2 ms. The wavelengths of LDAs were chosen in such manner, that the average absorption coefficient was maintained at a level of $\alpha_{\text{eff}} \approx 4\ cm^{-1}$ in the temperature range of 15 °C ÷ 35 °C. The pump radiation was focused by two cylindrical YAG lenses (*Laser Components*) with focal length of $f = 4.87$ mm, resulting in two $11 \times 3.4\ mm^2$ pumping areas. Because of high gain, we applied an electro-optical Q-switching technique – a Glan-Taylor polarizer (GT) and a RTP Pockels cell ($5 \times 5 \times 20\ mm^3$,

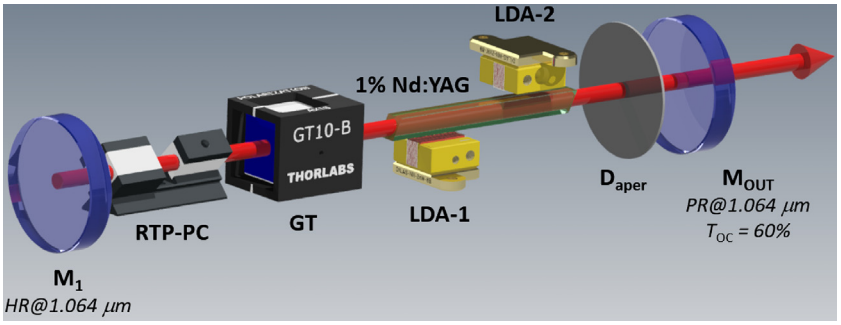

Fig. 8. The Nd:YAG slab laser resonator scheme. M_{out} – output mirror, M_1 – rear mirror, RTP-PC – pockels cell, GT – Glan polariser, LDA – laser diode array, D_{aper} – aperture stop.

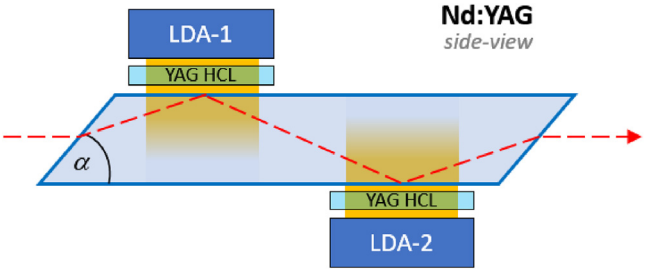

Fig. 9. Nd:YAG side-view with two TIR: YAG HCL – horizontal cylindrical lens made of YAG, LDA – laser diode array.

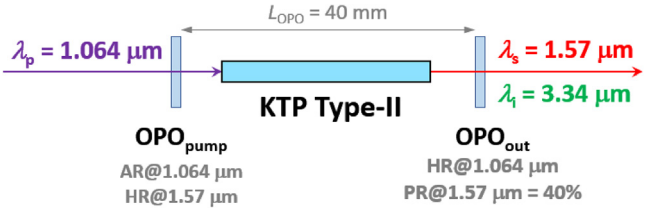

Fig. 10. The single resonance OPO cavity scheme.

Y-axis, $U_{\lambda/4}$ = 1.1 kV; *Cristal Laser*). To filter out the higher-order modes, we put a circular aperture with diameter D_{aper} = 3 mm next to output coupler. The resonator length was equal to L_{rez} = 340 mm.

The single-resonance OPO resonator (SRO) is shown in Fig. 10.

The SRO length was equal L_{SRO} = 40 mm. The cavity was formed by two plane-parallel mirrors (*Crytur*). The outcoupling transmission of mirror OPO_{out} was 40%. The KTP Type-II (o-oe, $\theta = 90^\circ, \varphi = 0^\circ$) used in research had dimensions of $4 \times 4 \times 35\ mm^3$.

4. Results

The pump duration time was set to t_p = 0.2 ms and repetition frequency was f_{rep} = 20 Hz. The active medium temperature was maintained at 35 °C. The outcoupling transmission was T_{OC} = 60%. The energetic characteristics measured in a free-running operation are shown in Fig. 11.

The empty resonator (without Q switching valve) generated 177 mJ of energy with slope efficiency 28.4%. The Glan-Taylor polarizer and RTP Pockels cell were put into the cavity introducing intrinsic losses. The generated output slightly dropped to 150 mJ. In the next step, we measured Q-switching generation parameters.

For total pump energy of 770 mJ (two LDAs) we have obtained single pulse generation with energy of 55 mJ and pulse width of 15 ns, what corresponds to 3.7 MW of pulse peak power However, above 400 mJ of pump energy, strong ASE began to manifest, significantly limiting gain. The experiment was repeated with a single LDA (second one was turned off), but the ASE was not supressed

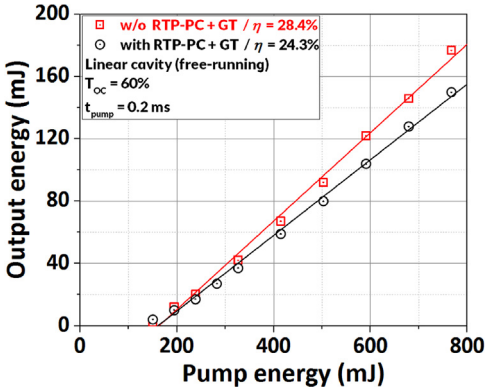

Fig. 11. Energetic characteristics of qcw operation.

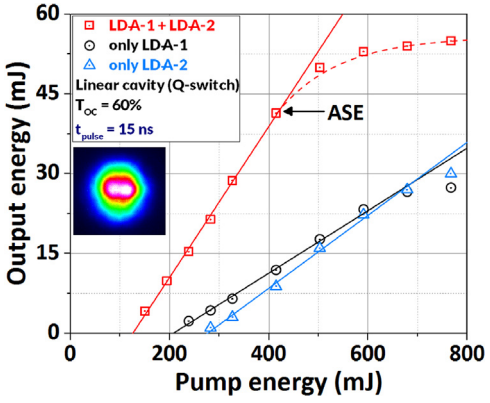

Fig. 12. Energetic characteristics of Q-switched operation – red dashed-line shows an influence of ASE limiting output pulse energy.

(see Fig. 12). Figure 13 shows generation time trace with visible ASE for the maximum pump energy of 770 mJ. We did not observe any "leakage" from Pockels cell.

We think it is not possible to achieve more than 25 mJ of pulse energy in Q-switching operation, from a laser head pumped by a single LDA. By extrapolating the linear part of the energetic characteristics, that in the absence of ASE, we expect to obtain 100 mJ of energy in a single pulse. For maximum pump energy, full-angle beam divergence was measured to be Θ = 2.5 mrad.

The energetic characteristics of parametric generation are shown in Fig. 14. For maximum pump energy, we achieved 28 mJ of signal wave (at 1.57 μm) energy with conversion efficiency η_{opo} = 51.3% in relation to pumping wave (at 1.064 μm). The pulse duration was measured to be 20 ns. It corresponds to 1.4 MW of pulse peak power. Figure 15 shows the time trace of an OPO signal wave pulse.

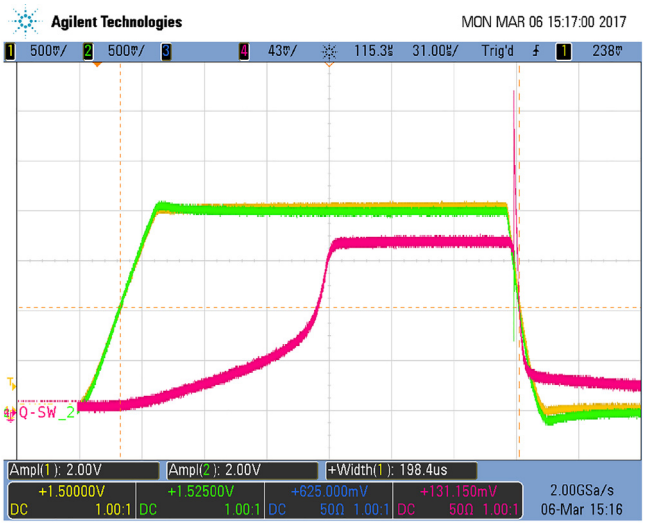

Fig. 13. The Q-switched operation time trace (pink) with visible ASE part – two background traces (green and yellow) represent pump radiation.

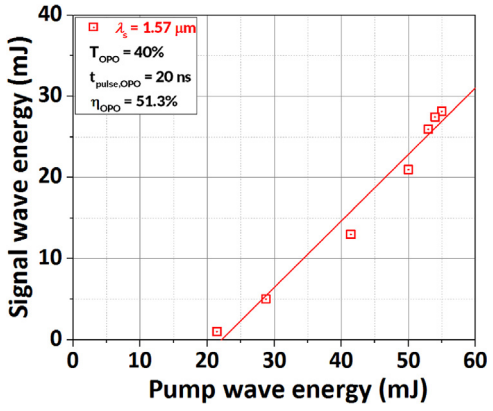

Fig. 14. Energetic characteristics of KTP-OPO.

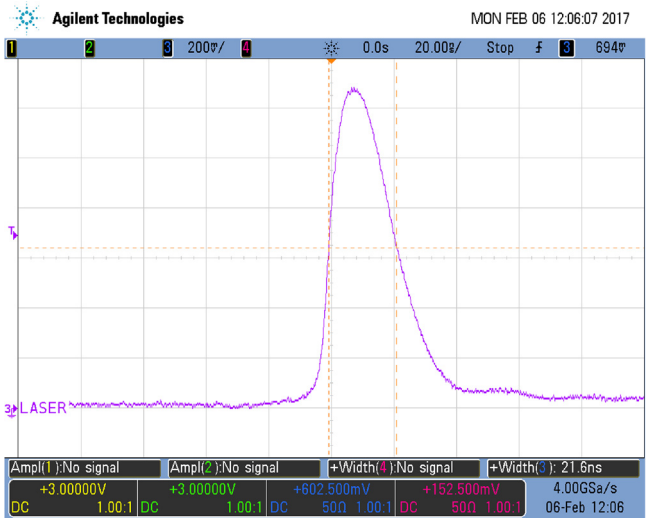

Fig. 15. An OPO signal wave pulse (λ_s = 1.57 μm) time trace.

5. Conclusions

We demonstrated at 28 mJ KTP-OPO "eye-safe" transmitter with a pulse peak power of 1.4 MW. The main factor limiting achievable high output energy is an amplified spontaneous emission. This phenomenon occurred at LDAs pump energy of 400 mJ (half available) causing significant roll-off of the energetic characteristics. To generate higher energy output and to supress ASE in Q-switched operation, one should use more pumping units located along the gain-medium (for instance if we use 4 LDAs, we should achieve about 100 mJ of single pulse energy) or implement master oscillator power amplifier architecture. In our preliminary experiments with Nd:YAG MOPA system, we obtained 155 mJ of pulse energy in Q-switched operation. We expect in near future to generate 100 mJ of "eye-safe" radiation.

Acknowledgement

This research was supported by Polish National Centre for Research and Development under Project No. PBS/B3/27/2015 ID 245812.

References

[1] M. Michalska, J. Swiderski, Highly efficient, kW peak power, 1.55 μm all-fiber MOPA system with a diffraction-limited laser output beam, Appl. Phys. B 117 (2014) 841–846.
[2] Z. Zhao, H. Xuan, H. Igarashi, S. Ito, K. Kakizaki, Y. Kobayashi, Single frequency, 5 ns, 200 μJ, 1553 nm fiber laser using silica based Er-doped fiber, Opt. Express 23 (2015) 29764–29771.
[3] S. Bigotta, K. Diener, M. Eichhorn, L. Galecki, L. Geiss, T. Ibach, H. Scharf, M. Von Salisch, J. Schoner, G. Vincent, Investigation on scalable high-power lasers with enhanced 'eye-safety' for future weapon systems, in: Proc. SPIE 9990, High-Power Lasers 2016: Technology and Systems, 999003, 2016.
[4] L. Galecki, M. Eichhorn, W. Zendzian, Pulsed 1.645 μm Er^{3+}:YAG laser with increased average output power and diffraction limited beam quality, Laser Phys. Lett. 10 (2013) 105813.
[5] W. Zendzian, J. Jabczynski, J. Kwiatkowski, Intracavity optical parametric oscillator at 1572-nm wavelength pumped by passively Q-switched diode-pumped Nd:YAG laser, Appl. Phys. B 76 (2003) 355–358.
[6] C.Y. Cho, Y.C. Chen, Y.P. Huang, Y.J. Huang, K.W. Su, Y.F. Chen, High-repetition-rate quasi-CW side-pumped mJ eye-safe laser with a monolithic KTP crystal for intracavity optical parametric oscillator, Opt. Express 22 (2014) 7625–7631.
[7] H. Chu, J. Zhao, T. Li, S. Zhao, K. Yang, D. Li, G. Li, W. Qiao, Y. Sang, H. Liu, KTP OPO with signal wave at 1630 nm intracavity pumped by an efficient σ-polarized Nd,MgO:LiNbO3 laser, Opt. Mater. Express 5 (2015) 684–689.
[8] W. Zendzian, J. Jabczynski, P. Wachulak, J. Kwiatkowski, High-repetition-rate, intracavity-pumped KTP OPO at 1572 nm, Appl. Phys. B 80 (2005) 329–332.
[9] Crystals for RGB Lasers – company catalogue Qingdao Crystech E&O Co. 2003–2004 http://www.crystech.com.
[10] J.D. Bierlein, H. Venherzeele, A.A. Ballman, Linear and nonlinear optical properties of flux-grown $KTiOAsO_4$, Appl. Phys. Lett. 54 (1989) 783–785.
[11] K. Kato, Parametric oscillation at 3.2 μm in KTP Pumped at 1.064 μm, IEEE J. Quantum Electron. 27 (1991) 1137–1140.
[12] M. Born, E. Wolf, Principles of Optics, Permagon, Oxford, 1970.
[13] F. Ratajczyk, Optyka Ośrodków Anizotropowych, PWN, Warszawa, 1994.
[14] R.D. Stultz, M.E. Ehritz, E. Segundo, Temperature (−32 °C to +90 °C) performance of a 20 Hz potassium titanyl phospate optical parametric oscillator, Adv. Solid State Lasers OSA TOPS 1 (1996) 147–149.
[15] Crystals & Materials, Casix, Crystal Guide 2000 http://www.casix.com.
[16] P. Chmela, Wprowadzenie do optyki nieliniowej, PWN, Warszawa, 1987.
[17] D.A. Roberts, Simplified characterization of uniaxal and biaxial nonlinear optics crystal: a plea for standardization of nomenclature and conventions, IEEE J. Quantum Electron. 28 (1992) 2057–2073.
[18] J.Q. Yao, T.S. Fahlen, Calculations of optimum phase match parameters for the biaxial crystal $KTiOPO_4$, J. Appl. Phys. 55 (1984) 65–68.